

---

# MagicTime: Time-lapse Video Generation Models as Metamorphic Simulators

---

Shenghai Yuan<sup>1,\*</sup>, Jinfa Huang<sup>2,\*</sup>, Yujun Shi<sup>3</sup>, Yongqi Xu<sup>4</sup>, Ruijie Zhu<sup>5</sup>,  
Bin Lin<sup>1</sup>, Xinhua Cheng<sup>1</sup>, Li Yuan<sup>1,†</sup>, Jiebo Luo<sup>2</sup>

\* Equal Contributors, † Corresponding Author

Code and Dataset: <https://github.com/PKU-YuanGroup/MagicTime>

<sup>1</sup> Peking University, Shenzhen Graduate School, <sup>2</sup> University of Rochester,

<sup>3</sup> National University of Singapore, <sup>4</sup> Guangdong University of Technology,

<sup>5</sup> University of California Santa Cruz

{chengxinhua@stu., yuanli-ece@, 2301212775@stu}pku.edu.cn,

{shyuan.x.cs, yongqixuing}@gmail.com, shi.yujun@u.nus.edu,

rzhu48@ucsc.edu, {jhuang90@ur, jluo@cs}.rochester.edu

## Abstract

Recent advances in Text-to-Video generation (T2V) have achieved remarkable success in synthesizing high-quality general videos from textual descriptions. A largely overlooked problem in T2V is that existing models have not adequately encoded physical knowledge of the real world, thus generated videos tend to have limited motion and poor variations. In this paper, we propose **MagicTime**, a metamorphic time-lapse video generation model, which learns real-world physics knowledge from time-lapse videos and implements metamorphic generation. First, we design a MagicAdapter scheme to decouple spatial and temporal training, encode more physical knowledge from metamorphic videos, and transform pre-trained T2V models to generate metamorphic videos. Second, we introduce a Dynamic Frames Extraction strategy to adapt to metamorphic time-lapse videos, which have a wider variation range and cover dramatic object metamorphic processes, thus embodying more physical knowledge than general videos. Finally, we introduce a Magic Text-Encoder to improve the understanding of metamorphic video prompts. Furthermore, we create a time-lapse video-text dataset called **ChronoMagic**, specifically curated to unlock the metamorphic video generation ability. Extensive experiments demonstrate the superiority and effectiveness of MagicTime for generating high-quality and dynamic metamorphic videos, suggesting time-lapse video generation is a promising path toward building metamorphic simulators of the physical world. <sup>1</sup>

## 1 Introduction

Recent advances in Text-to-Video (T2V) generation models have been driven by the emergence of diffusion models. These models are typically based on either Transformer architectures [2, 3] or U-Net architectures [4, 5, 6, 1]. The former approach tokenizes videos and incorporates positional encoding for training, whereas the latter extends the 2D U-Net with a temporal feature extraction module for pseudo-3D training. However, the videos generated by these models primarily exhibit camera movement, lacking a continuous subject metamorphic process and limited incorporation of physical knowledge. We categorize such videos as *general videos*, illustrated in Fig. 1a. Since the

---

<sup>1</sup>Our project aims to help reproduce [Sora](#), supporting [Open-Sora-Plan](#) or other DiT-based T2V models.

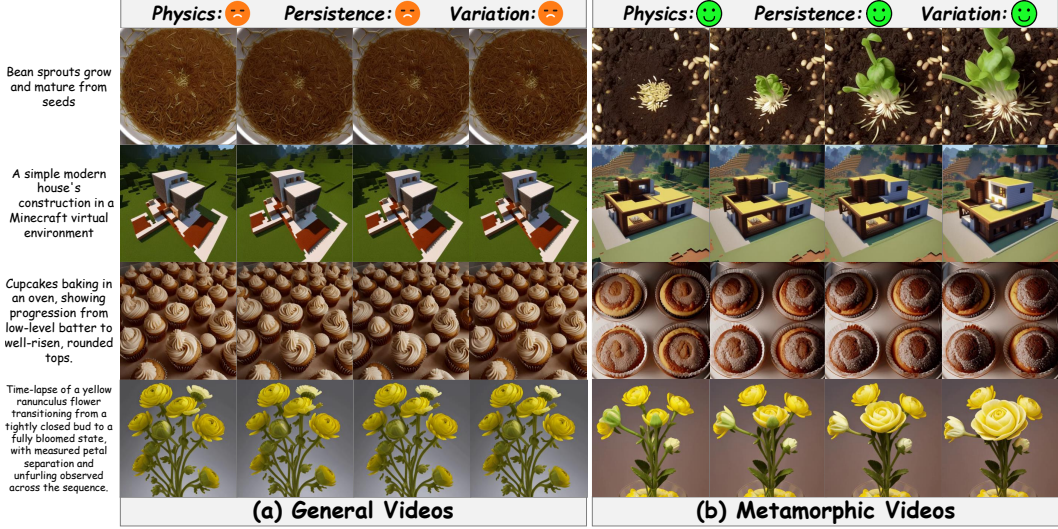


Figure 1: **The illustration of the difference between (a) general videos, and (b) metamorphic videos.** Compared to general videos, metamorphic videos contain physical knowledge, long persistence, and strong variation, making them difficult to generate. The general videos are generated by the Animatediff [1]. Our MagicTime greatly improves capabilities of metamorphic video generation.

training datasets predominantly consist of general videos, current T2V models struggle to produce videos depicting complex phenomena like seed germination, ice melting, or flower blooming, which are characterized by minimal physical content, brief duration, and limited variation.

Compared to general videos, we have observed a category of videos that typically encompasses the subject’s entire transformation process, thus addressing the inherent limitations of the former. We term this category as *metamorphic videos*, which encode a more comprehensive representation of world knowledge, as illustrated in Fig. 1b. Such videos have the potential to enhance the capacity of video generation models to accurately depict the real world. Consequently, the generation of metamorphic videos is of paramount importance for a wide range of applications, despite being relatively underexplored in existing research. While the study [7] demonstrates the ability to create similar effects by repeatedly inferring and concatenating general videos, it falls short in encoding physical knowledge and lacks generalization through a prompt strategy. In contrast, we aim to develop an end-to-end time-lapse video generation method for adaptively encoding physical knowledge with good generalization.

Time-lapse videos provide detailed documentation of an object’s complete metamorphosis, possessing the essential characteristics of metamorphic videos. Consequently, we utilize time-lapse videos to validate our hypothesis. A straightforward approach is to leverage existing powerful T2V models to directly generate metamorphic videos. Since metamorphic videos and general videos have intrinsic gaps, current methods struggle to produce satisfactory metamorphic videos directly. The core challenges include: (1) Metamorphic time-lapse videos contain more physics, requiring stronger structural extraction; (2) It has longer persistence, fully covering object metamorphosis and being sensitive to training strategies; (3) Metamorphic time-lapse videos have greater variation, potentially transforming from seed to flower, demanding high-quality data.

To tackle the challenge of generating metamorphic videos, we introduce a novel framework, **MagicTime**, which excels in creating video content that is **Magically** compressed in **Time**. Initially, we present the MagicAdapter to encode more physical knowledge in metamorphic videos into the feature extraction, expanding the metamorphic video generation capabilities of pre-trained T2V models without altering their core general video generation abilities. Subsequently, we propose a Dynamic Frames Extraction strategy that enables the model to adapt to the characteristics of time-lapse training videos and prioritize metamorphic video features. Moreover, we introduce a Meta Text-Encoder to refine prompt understanding and distinguish between metamorphic and general prompts. As shown in Fig. 1b, our MagicTime generates text-aligned, coherent, high-quality metamorphic videos across various styles, coordinated with carefully designed techniques.

Table 1: **Comparison of the characteristics of our ChronoMagic benchmark with existing time-lapse datasets.** We compare time-lapse video characteristics in terms of physics, persistence, and variation.

Dataset	Type	Strong Physics	High Persistence	Variation
Sky Time-Lapse <small>[ACMMM'21]</small> [8]	General	✗	✗	✗
Time-Lapse-D <small>[CVPR'18]</small> [9]	General	✗	✗	✗
ChronoMagic	Metamorphic	✓	✓	✓

Further, we meticulously collect a dataset, ChronoMagic, sourced from Internet time-lapse videos for training our method. As shown in Table 1, our ChronoMagic dataset is distinct from previous time-lapse datasets [8, 9], as it consists of metamorphic time-lapse videos (e.g. ice melting, and flower blooming) that show strong physics, high persistence, and variation. Given the domain discrepancy between metamorphic and general videos, we propose the integration of Cascade Preprocessing and Multi-View Text Fusion to capture dynamics into detailed video captions. Contributions are summarized as follows:

- We introduce **MagicTime**, a metamorphic time-lapse video generation diffusion model by adopting a standard T2V model with a MagicAdapter scheme. This addresses the limitations of existing methods that are unable to generate metamorphic videos.
- We design a Dynamic Frames Extraction strategy to effectively extract physics from metamorphic videos and a Magic Text-Encoder to enhance the model’s understanding of metamorphic text prompts.
- We propose an automatic metamorphic video captioning annotation framework. Utilizing this framework, we have curated a high-quality dataset named **ChronoMigic**, consisting of 2,265 time-lapse videos, each accompanied by a detailed caption.
- Extensive experiments demonstrate that our **MagicTime** is capable of generating high-quality and consistent metamorphic time-lapse videos.

## 2 Related Work

**Text-to-Image Generation** Text-to-image (T2I) synthesis has made significant strides thanks to advancements in deep learning and the availability of large image-text datasets such as CC3M [10] and LAION [11]. Compared to variational autoencoders (VAEs) [12, 13], flow-based models [14, 15], and generative adversarial networks (GANs) [16, 17, 18], diffusion models [19, 20, 21, 22, 23, 24] have demonstrated exceptional efficacy in image modeling. For instance, contemporary T2I models often employ Latent Diffusion Models (LDM) [25], which utilize sampling in latent spaces from pre-trained autoencoders to minimize computational overhead. Recapti [26] harnessed the power of Large Language Models (LLM) to improve the text comprehension capabilities of LDM, enabling training-free T2I generation. Furthermore, the integration of additional control signals [27, 28, 29, 30, 31] has further expanded the applicability of Diffusion Models in T2I synthesis. Unlike image generation, the task of video generation required by MagicTime is more complex, as it necessitates both diversity in content across space and consistency in content across time.

**Text-to-Video Generation** The advent of large-scale video-text datasets [32, 33, 34] has facilitated significant advancements in pre-trained video diffusion models [35, 36, 6, 37, 5, 38]. MagicVideo2 [39] utilized cascaded diffusion to separate image and video generation, starting with text to initially generate images and subsequently produce high-quality videos. Videopoet [2] employed a Transformer-based diffusion approach, combined with multimodal inputs, for zero-shot video generation. Animatediff [1] and Lumiere [40] extended the 2D-UNet to a 3D-UNet by adding temporal layers and implementing a latent denoising process to conserve computational resources. While these models have achieved basic video generation, the resulting videos typically feature a single scene and a single action, and lack encoding of physical world knowledge. In contrast, our MagicTime incorporates more physics knowledge and offers the capability to generate metamorphic videos.

**Time-lapse Video Generation** Previous studies [41, 42, 43, 44] on time-lapse video generation predominantly concentrated on general videos, failing to produce the metamorphic videos that we

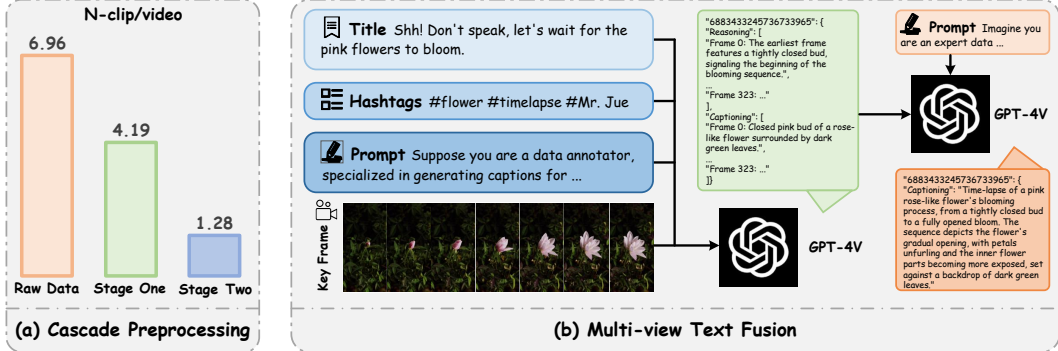


Figure 2: **The pipeline for high-quality time-lapse video data annotation.** (a) **Cascade Preprocessing.** We successfully detect many useless cuts. The results are obtained by OpenCV. (b) **Multi-view Text Fusion.** Compared with only inputting keyframes, our pipeline can obtain vivid, detailed and accurate descriptions.

address. For example, [42, 43] treated time-lapse videos merely as a distinct domain, overlooking the physical knowledge embedded within them. Consequently, the generated videos were limited to scenes with relatively minor movements, such as drifting clouds or moving sunsets. In contrast, our work primarily focuses on generating metamorphic time-lapse videos, which exhibit larger variations and depict the entire process of object metamorphosis. In this work, we aim to incorporate more physical knowledge into MagicTime for metamorphic time-lapse video generation.

### 3 Methodology

In this section, we commence with a brief overview of the latent diffusion model. Subsequently, we describe the construction of the ChronoMagic dataset. Lastly, we present an outline of MagicTime (refer to Fig. 3) and elaborate on its implementation details.

#### 3.1 Preliminaries

Diffusion models [45, 46] typically consist of two processes: forward diffusion and reverse denoising. Given an input signal  $x_0$ , the process of forward diffusion is defined as follows:

$$p_{\theta}(x_t | x_{t-1}) = \mathcal{N}\left(x_t; \sqrt{1 - \beta_t}x_{t-1}, \beta_t I\right), \quad (1)$$

where  $t = 1, \dots, T$  are time steps, and  $\beta_t \in (0, 1)$  is the noise schedule. When the total time steps  $T$  are sufficiently large, the resulting  $x_t$  eventually approximates Gaussian noise  $\in N(0, I)$ . The purpose of the denoising process is to learn how to reverse the forward diffusion and gradually remove the noise as follows:

$$p_{\theta}(x_{t-1} | x_t) = \mathcal{N}(x_{t-1}; \mu_{\theta}(x_t, t), \Sigma_{\theta}(x_t, t)), \quad (2)$$

where  $\Sigma_{\theta}(x_t, t)$  often does not need to be trained but is calculated based on the time step  $t$  as a fixed variance. It only needs to predict the mean  $\mu_{\theta}(x_t, t)$  in the reverse process, and this step can also be simplified to training the denoising model  $\epsilon_{\theta}(x_t, t)$  to predict the noise  $\epsilon$  of  $x_t$ :

$$\mathcal{L} = \mathbb{E}_{y, \epsilon \sim \mathcal{N}(0, I), t} \left[ \|\epsilon - \epsilon_{\theta}(x_t, t, \tau_{\theta}(y))\|_2^2 \right], \quad (3)$$

where  $y$  is text condition, and  $\tau_{\theta}(\cdot)$  is the text encoder. By replacing  $x_0$  with  $\mathcal{E}(x_0)$ , the latent diffusion model is derived, which also serves as the loss function for MagicTime. In video diffusion models, the parameter  $\theta$  typically employs either a Transformer [2, 3] or a U-Net architecture [4, 5, 6, 1, 47]. Considering that the most effective open-source T2V models currently utilize U-Net architecture, we have embraced this architecture in this work.

#### 3.2 ChronoMagic Dataset

**Data Curation and Filter** We found that videos in large-scale text-video datasets like WebVid [32] typically consist of coherent segments depicting everyday life (general videos), devoid of significant

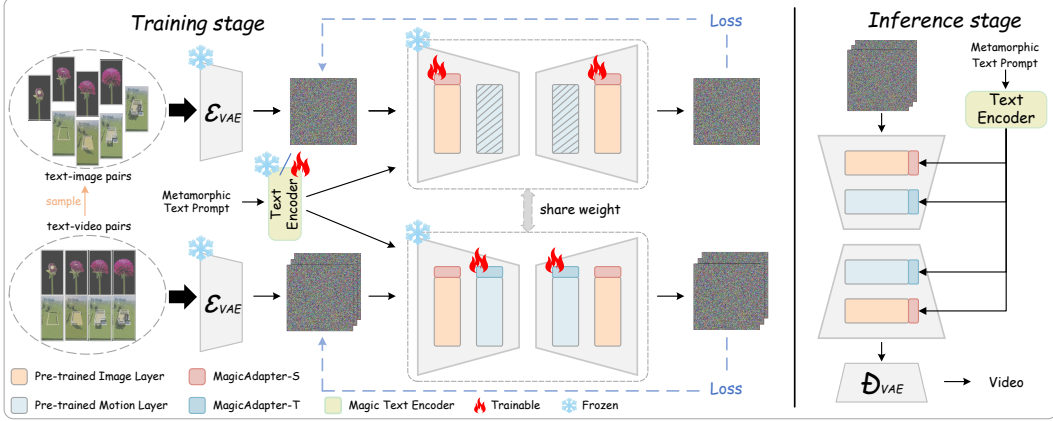


Figure 3: **Overview of the proposed MagicTime approach.** We first train *MagicAdapter-S* to remove the influence of watermarks. Next, *MagicAdapter-T* is trained to generate metamorphic videos with the help of *Dynamic Frames Extraction*. Finally, we train a *Magic Text-Encoder* to enhance text comprehension ability. During the inference stage, all components need to be loaded simultaneously. Slash padding indicates the module is not used.

changes or object metamorphosis. Consequently, open-source models [36, 35, 1] are limited to generating general videos and are unable to produce metamorphic videos. To overcome this limitation, we introduce the ChronoMagic dataset, which includes 2,265 high-quality time-lapse videos with accompanying text descriptions from open-domain content. Time-lapse videos capture complete object metamorphosis and convey more physical knowledge than general videos, thereby enhancing generative models’ understanding of the world.

Given that video platforms host a multitude of low-quality videos, indiscriminate collection would inevitably compromise the dataset’s quality. To mitigate this, we leverage the metadata from video websites for collection and filtering. Our data collection process begins with retrieving original videos from YouTube using "time-lapse" as a search term. Subsequently, we implement a filtering mechanism that excludes videos with short titles, low view counts, or absent hashtags. Furthermore, we discard videos with irrelevant hashtags such as "YouTube," "video," and "shorts." Building on the annotations generated in Section 3.2, we further refine our selection by eliminating irrelevant videos, thus establishing a closed-loop data collection and iteration process. Ultimately, we curate a collection of 2,265 time-lapse videos that meet our specified criteria.

**Cascade Preprocessing** Due to complex scene transitions in original videos (see Fig. 2a) affecting the model’s learning of temporal relevance, we need to find a way to solve this problem. The most direct method is to use existing tools for detection, so we choose OpenCV [48] as a tool. In the initial stage, we define  $F$  as the set of all video frames. Each frame  $f_i$  in  $F$  is converted to grayscale  $g_i \in (1, H, W)$  to mitigate the influence of color on detection. Subsequently, OpenCV is used to calculate the pixel intensity difference  $\mathcal{D}_{i,i+1}$  between consecutive frames, yielding the average pixel intensity  $\mathcal{S}_{i,i+1}^{opencv}$ :

$$\mathcal{D}_{i,i+1} = |g_i - g_{i+1}|, \quad \text{for } i = 1 \text{ to } F - 1 \quad (4)$$

$$\mathcal{S}_{i,i+1}^{opencv} = \sum_{h=1}^H \sum_{w=1}^W \mathcal{D}_{i,i+1}(h, w), \quad \text{for } i = 1 \text{ to } F - 1 \quad (5)$$

if  $\mathcal{S}_{i,i+1}^{opencv} > \theta$ , then this position is defined as the transition point. However, we noted that OpenCV is prone to occasional errors. Consequently, we further employ CLIP [49] to detect differences between frames:

$$\mathcal{S}_{i,i+1}^{clip} = \cos(\text{CLIP}(f_i), \text{CLIP}(f_{i+1})), \quad \text{for } i = 1 \text{ to } F - 1 \quad (6)$$

if  $\mathcal{S}_{i,i+1}^{clip} < \vartheta$ , then this position is defined as the transition point. The  $\cos(\cdot)$  returns a similarity vector. After that, we use a voting mechanism to decide whether a specific location should be recognized as

a transition point:

$$\mathcal{T}_i = \begin{cases} \text{True,} & \text{if } \mathcal{S}_{i,i+1}^{opencv} > \theta \text{ and } \mathcal{S}_{i,i+1}^{clip} < \vartheta \\ \text{False,} & \text{otherwise} \end{cases} \quad (7)$$

where  $i$  represents the position of the frame. Ultimately, we segment the video into distinct sections using the identified transition points. Due to possible detection errors in OpenCV and CLIP, the video may still contain transitions that are challenging to identify after processing. In the subsequent stage, we enhance video quality by manually correcting incorrectly cropped segments and then screening clean segments. As illustrated in Fig. 2a, the process results in a high-quality video dataset with fewer transitions.

**Multi-view Text Fusion** After preprocessing, it is essential to annotate the video with appropriate captions. A straightforward approach is to input keyframes into a multimodal model for video description. However, the absence of substantial intermediate information may compromise the quality of the annotations. The ChronoMagic dataset’s language modality includes multiview text, such as titles, hashtags, keyframe captions, and video captions, so we leverage these to enhance labeling accuracy. Fig. 2b shows the detailed text generation and fusion process. In videos, titles underscore main themes and actions, while hashtags highlight focus and dynamics. Theoretically, high-quality captions could be generated solely from titles and hashtags. Nevertheless, exaggerated titles and hashtags on the internet can diminish caption quality. To counteract this, we employ in-context Learning and Chain-of-Thought [50] to guide GPT-4V [51, 52] in generating keyframe captions using titles and hashtags, thereby reducing model bias and capturing spatial video information. Moreover, temporal video information is crucial. Thus, we use GPT-4V to derive a comprehensive representation of the entire video from keyframe captions, resulting in the final video captions. Additionally, at this stage, GPT-4V evaluates whether the video is a time-lapse and then forms a closed data loop as described in Section 3.2.

### 3.3 MagicTime Model

**MagicAdapter** To transform the pre-trained T2V model to generate metamorphic videos, we decouple the training process into two stages: spatial training and temporal training, refer to Fig. 3.

Internet video data often contains non-removable watermarks, introducing irrelevant noise and data bias. Video generation models consist of spatial and temporal layers—the former focuses on learning visually relevant content, while the latter builds inter-frame continuity. If we can separate temporal and spatial training, allowing the spatial module to concentrate more on the subject rather than the watermark, this will facilitate the temporal layer in learning the motion patterns of metamorphic videos. To accomplish this, in the initial training phase, we remove the temporal layer from the pre-trained model and integrate the MagicAdapter-S into the spatial layer, inspired by QLoRA Adapter [53]. Subsequently, we freeze the remaining model parameters and employ keyframe-text pairs from the ChronoMagic dataset for training. Formally, let input  $X$  to a single spatial layer  $\mathcal{F}_{sap}$  and MagicAdapter-S layer  $\mathcal{R}_{ada}$  be in the form  $\mathbb{R}^{B \times C \times H \times W}$ . The output of this layer is:

$$\mathcal{F}_{out}(X) = \mathcal{F}_{sap}(X) + \alpha \times \mathcal{R}_{ada}(X), \quad (8)$$

where  $\mathcal{F}_{out} \in \mathbb{R}^{B \times C \times H \times W}$ , and  $\alpha$  is a scaling coefficient used to regulate the scope of the adapter.  $B$ ,  $C$ ,  $F$ ,  $H$ , and  $W$  respectively represent the batch size, channel, number of frames, height, and width of the video. Ensuring high temporal consistency is crucial for video generation models. While general videos require consistency within localized segments, metamorphic videos necessitate consistency throughout the entire video, capturing a completely metamorphic process. Training alongside general videos could hinder the model’s comprehension of the new world phenomena. To mitigate this, we separate the training of general and metamorphic videos, thereby maintaining the model’s ability to generate general videos. Specifically, in the second training stage, we reintroduce the pre-trained temporal layer from the first stage, freeze all parameters, and propose a MagicAdapter-T into the temporal layer. Subsequently, we freeze other parameters and conduct training using video-text pairs from the ChronoMagic dataset. If the input  $X$  to a single temporal layer  $\mathcal{F}_{temp}$  and MagicAdapter-T layer  $\mathcal{M}_{ada}$  is in the form of  $\mathbb{R}^{B \times C \times F \times H \times W}$ , then the output of this layer is given by:

$$\mathcal{F}_{out}(X) = \mathcal{F}_{temp}(X) + \beta \times \mathcal{M}_{ada}(X), \quad (9)$$

where  $\mathcal{F}_{out} \in \mathbb{R}^{B \times C \times F \times H \times W}$ ,  $\beta$  is a scaling coefficient, and  $B$ ,  $C$ ,  $F$ ,  $H$ , and  $W$  respectively represent the batch size, channel, number of frames, height, and width of the video. Based on large-scale video-text data [32], the pre-trained model incorporates general motion capabilities [1] through

Table 2: Comparison of statistics among Sky Time-lapse [8], Time-lapse-D [9], and the proposed metamorphic ChronoMagic dataset. ChronoMagic is the only high-quality dataset for text-to-video generation tasks.

	ChronoMagic	Sky Time-lapse [8]	Time-lapse-D [9]
<b>Type</b>	Video-Text	Video	Video
<b>Clips</b>	2,265	2,049	16,874
<b>Resolution</b>	1280 × 720	640 × 360	1920 × 1080

its temporal layer. MagicAdapter-T further enhances the model’s ability to generate metamorphic videos by integrating physical knowledge and predicting metamorphic motion.

**Dynamic Frames Extraction** Open-source algorithms, whether for video generation [54, 55] or multimodal models [56, 57], typically sample a random continuous sequence of  $N$  frames for training. However, this approach captures only a brief segment of the full video, leading to limitations such as monotonous actions and restricted variation in amplitude. This is not conducive to extracting training frames for metamorphic videos. By analyzing ChronoMagic’s characteristics, we opt to sample  $N$  frames evenly from a video, capitalizing on the nature of metamorphic videos that encompass the entire process of object metamorphosis. This ensures that the training data exhibit metamorphic properties, rather than being confined to general ones, thereby enhancing the generative models’ ability to comprehend physical phenomena. Nonetheless, uniform sampling from all videos might compromise the model’s original capabilities, resulting in generated videos that lack the action continuity of general videos. Consequently, we retain a portion of general videos and dynamically select the sampling strategy based on the results of cascade preprocessing:

$$\mathcal{S}^* = \begin{cases} \text{Uniform, with } \mathcal{P}, & \text{if } \sum_{i=1}^{F-1} \mathcal{T}_i > \delta \\ \text{Random, with } \mathcal{P}, & \text{if } \sum_{i=1}^{F-1} \mathcal{T}_i \leq \delta \end{cases} \quad (10)$$

where probability  $\mathcal{P}$  represents the likelihood of executing the corresponding sampling strategy, enhancing model robustness.  $\delta$  represents the threshold for judging transition.

**Magic Text-Encoder** Textual descriptions corresponding to metamorphic videos typically contain more temporal and state information than those for general videos. Consequently, using a text encoder trained exclusively on general videos is deemed insufficient for this purpose. To overcome this limitation, we introduce the Magic Text-Encoder, which is specifically designed to encode metamorphic prompts while retaining its ability to process general prompts. We select CLIP as our initial text encoder and incorporate a Low-rank Adapter to encode metamorphic information. The training of the Magic Text-Encoder must be conducted after the overall network training is completed. Formally, given a projection  $\mathbf{X}\mathbf{W} = \mathbf{Y}$  with  $\mathbf{X} \in \mathbb{R}^{q \times w}$ ,  $\mathbf{W} \in \mathbb{R}^{w \times r}$ , adapter computes:

$$\mathbf{Y} = \mathbf{X}\mathbf{W} + \gamma\mathbf{X}\mathbf{L}_1\mathbf{L}_2, \quad (11)$$

where  $\mathbf{X}$  is the input,  $\mathbf{Y}$  is the output,  $\mathbf{L}_1 \in \mathbb{R}^{w \times e}$  and  $\mathbf{L}_2 \in \mathbb{R}^{e \times r}$  are adapter parameters,  $\mathbf{W}$  is CLIP parameters,  $\gamma$  is a scaling coefficient, and  $q, w, e, r$  are the dimensions of input, intermediate, low-rank, and output respectively. To avoid losing original capabilities, only  $\mathbf{L}_1$  and  $\mathbf{L}_2$  are updated.

## 4 Experiment

### 4.1 Experimental Settings

**Datasets** Metamorphic video generation represents a novel paradigm, yet dedicated evaluation datasets are scarce, presenting challenges for thorough method assessment. To address this need, we utilize the ChronoMagic dataset, the first benchmark specifically designed for metamorphic video generation. Detailed information and examples are provided in the Appendix. This dataset consists of high-quality metamorphic time-lapse videos with corresponding captions. The statistics of the ChronoMagic dataset are presented in Table 2.

**Metrics** In this work, we utilize three metrics for quantitative evaluation: Fréchet Inception Distance (FID) [63], Fréchet Video Distance (FVD) [64] and CLIP Similarity (CLIPSIM) [65]. These are

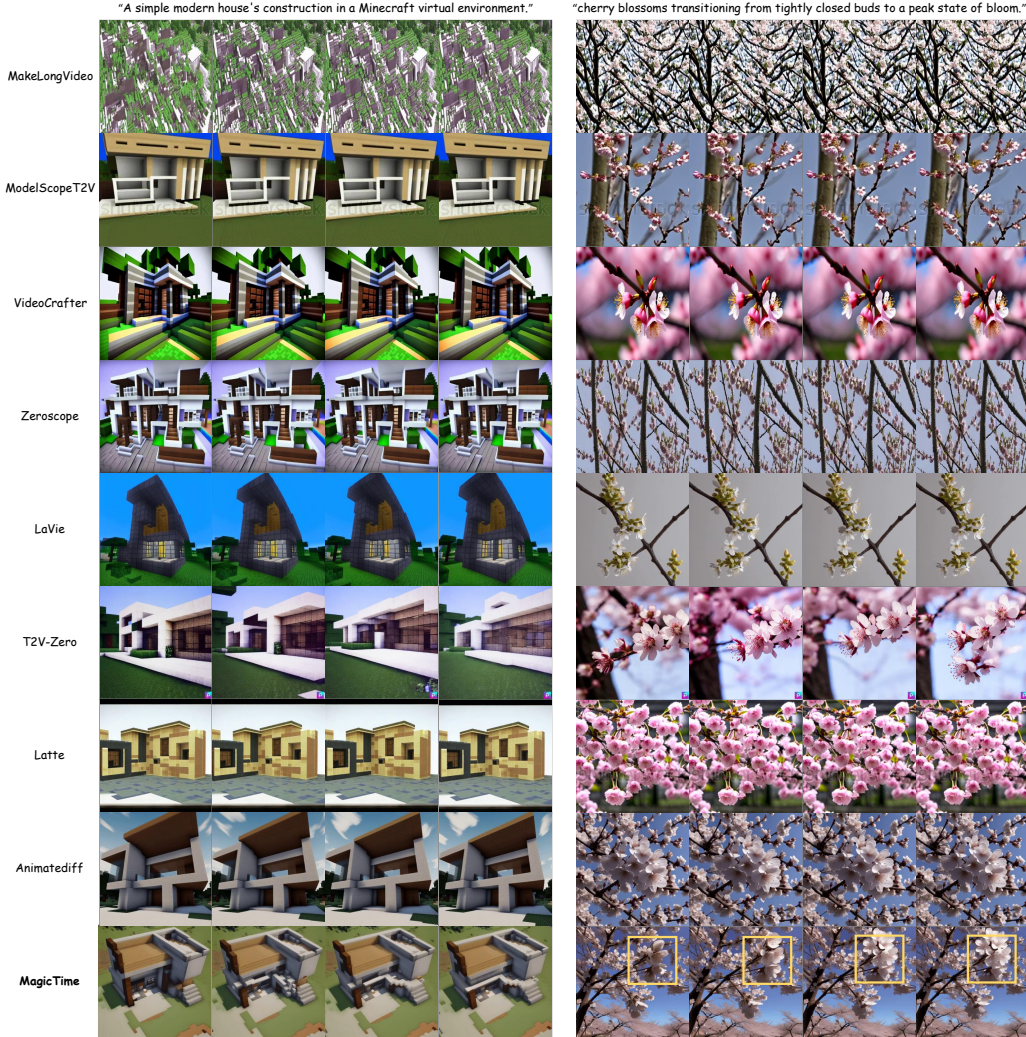


Figure 4: **Qualitative comparison for metamorphic video generation.** Among *MagicTime*, *Make-LongVideo* [58], *ModelScopeT2v* [5], *VideoCrafter* [59], *Zeroscope* [60], *LaVie* [61], *T2V-Zero* [62], *Latte* [3] and *Animatediff* [1], our *MagicTime* achieves the best results among all T2V models.

standard indicators assessing generated image quality, video quality, and text-content similarity. For a fair comparison, we set fixed random seeds in all experiments.

**Implementation Details** We choose Stable Diffusion v1.5 [25] and Motion Module v15 [1] as our baseline models. In the training stage, the resolution is set to  $512 \times 512$ , 16 frames are taken by Dynamic Frames Extraction from each video, the batch size is set to 1,024, the learning rate is set to  $1e-4$ , the total number of training steps is 10k, and the classify free guidance random null text ratio is 0.1. We use a linear beta plan as the optimizer with  $\beta_{\text{start}} = 8.5e - 4$  and  $\beta_{\text{end}} = 1.2e - 2$ . We set  $\theta$ ,  $\vartheta$ ,  $\mathcal{P}$  and  $\delta$  in Sections 3.2 and 3.3 to 40, 0.5, 0.9 and 3 respectively to enhance robustness. In the inference stage, we utilize DDIM with 25 sampling steps, a text-guided scale of 8.0, and a sampling size of  $512 \times 512$ . We have collected personalized SD models from CivitAI to verify the generalizability of our method, including Realistic Vision, RenzCartoon, and ToonYou. Due to space limitations, more qualitative experiments on generated metamorphic videos are shown in the Appendix. Further, selected examples from our ChronoMagic dataset, along with the questionnaire employed for human evaluation, are provided in the Appendix for further reference.



Figure 5: **Examples of our approach applied to generated metamorphic videos.** Metamorphic videos categories include *RealisticVision* (Row 1-3), *RcnzCartoon* (Row 4-6) and *ToonYou* (Row 7-9). Even with a large state amplitude, the quality, consistency, and semantic relevance of generated videos are excellent.

## 4.2 Qualitative Analysis

In this section, we first compare our method, MagicTime, with several state-of-the-art models including MakeLongVideo [58], ModelScopeT2V [5], VideoCrafter [59], Zeroscope [60], LaVie [61], T2V-zero [62], Latte [3], and Animatediff [1] in the task of metamorphic video generation. All input text is sourced from our ChronoMagic dataset. The evaluated tasks involve generating videos that depict significant metamorphosis, such as the construction of a modern house in Minecraft, the blooming of pink plum blossoms, the baking of bread rolls, and the melting of ice cubes, as shown in Fig. 4. Our evaluation focuses on Frame Consistency (FC), Metamorphic Amplitude (MA), and Text Alignment (TA). While all methods, except MakeLongVideo, produce high-quality videos with strong temporal modeling implied high FC, they struggle with TA and MA. The limited physical priors in existing text-to-video models restrict them to general scene generation, such as swaying flowers (ModelScopeT2V, VideoCrafter, Latte), static buildings (Zeroscope, LaVie, Animatediff, T2V-zero), which are incorrect contents. In contrast, MagicTime excels in capturing metamorphic transitions smoothly and accurately reflecting physical sequences, such as layer-by-layer Minecraft construction and natural flower blooming. Notably, MagicTime demonstrates the ability to generate visually consistent content over large time spans, accurately depicting processes like ice melting and dough baking, further validating the model’s effectiveness.

Table 3: **Quantitative comparison with state-of-the-art T2V generation methods for the text-to-video task.** Results are produced on ChronoMagic. Our method achieves either the best results or second-best results across all metrics. "↓" denotes lower is better. "↑" denotes higher is better.

Method	Venue	Backbone	FID↓	FVD↓	CLIPSIM↑
MakeLongVideo [58]	Github'23	U-Net	143.07	511.62	0.2852
ModelScopeT2V [5]	Arxiv'23	U-Net	61.49	500.43	0.3093
VideoCrafter [59]	CVPR'23	U-Net	<b>54.61</b>	473.69	0.3149
Zeroscope [60]	CVPR'23	U-Net	103.74	497.60	0.3079
LaVie [61]	Arxiv'23	U-Net	62.28	<u>445.60</u>	0.3090
T2V-zero [62]	ICCV'23	U-Net	58.58	488.85	<u>0.3203</u>
Latte [3]	Arxiv'24	DiT	59.10	445.85	0.2939
Animatediff [1]	ICLR'24	U-Net	63.83	451.35	0.3156
<b>MagicTime</b>	<b>Ours</b>	<b>U-Net</b>	<u><b>58.12</b></u>	<b>441.17</b>	<b>0.3272</b>

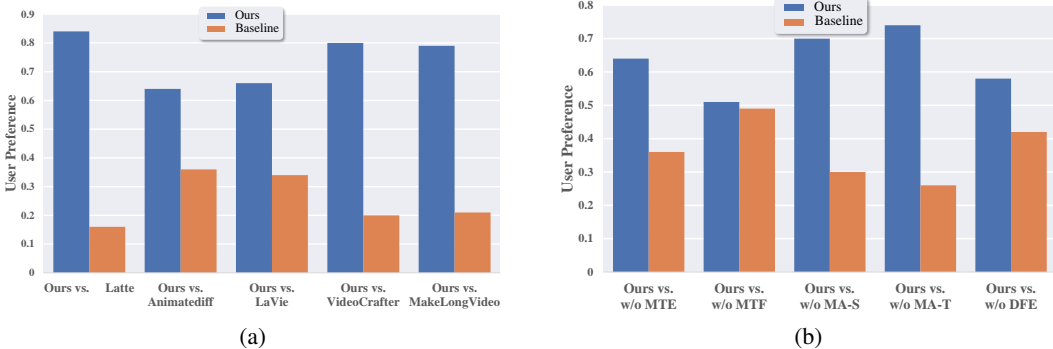


Figure 6: **(a) Human evaluation between MagicTime and state-of-the-art T2V generation methods.** MagicTime is preferred by human voters over other methods. **(b) Human evaluation of different ablation settings.** The most crucial components are *MagicAdapter-S/T* (MA-S/T) and *Dynamic Frames Extraction* (DFE), which empower MagicTime with metamorphic video generation capabilities. *Magic Text-Encoder* (MTE) and *Multi-view Text Fusion* (MTF) are primarily used to enhance video quality.

Next, to demonstrate the robustness and generality of our approach, we present several text-guided metamorphic video generation results. As shown in Fig. 5, MagicTime effectively converts a general T2V model into a metamorphic video generator, yielding impressive outcomes ranging from swelling and melting to growing and building. These results showcase a robust understanding of physical phenomena encoded within the model. Even when the textual prompt requires the generation of content spanning long periods, the generated videos maintain high quality, consistency, and semantic relevance. This success is attributed to our method of preserving image generation and temporal modeling priors learned from SD and T2V baselines on large datasets while encoding physical priors characteristic of metamorphic videos.

### 4.3 Quantitative Analysis

In this section, we conduct a comprehensive quantitative evaluation to assess the performance of our approach. We compare the generation quality on the ChronoMagic dataset between MagicTime and baseline methods, as presented in Table 3. Consistent with the results in Fig. 4, MakeLongVideo exhibits the highest FID and FVD values, indicating its inferior visual quality compared to other methods. While VideoCrafter has the lowest FID, our method boasts the lowest FVD, suggesting that MagicTime offers the highest video quality. CLIPSIM, originally applied in image generation, mainly measures the similarity between individual video frames and text for videos, which limits its effectiveness in assessing video generation quality. Given the lack of superior metrics in the T2V field, we use CLIPSIM as an indicator of video-text relevance. Numerically, although the video-text relevance of MagicTime is the highest, it is only slightly higher than the other methods. However, as shown in Fig. 4, only MagicTime adheres to the text prompt instructions to generate



Figure 7: **Ablation study for different parts of MagicTime.** It shows the effectiveness of *Magic Text-Encoder (MTE)*, *Multi-view Text Fusion (MTF)*, *MagicAdapter-S/T (MA-S/T)*, and *Dynamic Frames Extraction (DFE)*.

metamorphic videos, while the baseline methods generate general videos based on the theme of the prompt, implying that their CLIPSIM scores should be lower. Overall, our method surpasses all compared methods, confirming that in modeling metamorphic videos, we can ensure superior video generation quality while successfully incorporating more physical priors, thus producing results that align with the definition of metamorphic videos.

#### 4.4 Human Evaluation

As previously mentioned, metrics such as FID, FVD, and CLIPSIM may not fully capture the generative capabilities of T2V methods. To address this, we enlisted 200 participants to evaluate the Visual Quality, Frame Consistency, Metamorphic Amplitude, and Text Alignment of videos generated by MagicTime and baseline methods. We selected 15 sets of samples for each criterion and asked participants to choose the high-quality metamorphic video that best aligned with their expectations. For fairness, all options were randomized, and each participant could only complete one questionnaire under identical conditions. Due to the need for a large pool of participants in the evaluation, we only select the top 5 T2V methods for voting. We finally collected 185 valid questionnaires. The results, depicted in Fig. 6a, demonstrate that our method significantly outperforms other leading T2V methods. Furthermore, MagicTime significantly enhances the quality of metamorphic video generation, validating our approach’s effectiveness in encoding physical knowledge through training with metamorphic videos. Visualizations of the questionnaire are provided in the Appendix.

#### 4.5 Ablation Study

**Validation on Different Components** We primarily conduct ablation studies on our proposed strategies of Dynamic Frames Extraction (DFE), MagicAdapter-T (MA-T), MagicAdapter-S (MA-S), Multi-view Text Fusion (MTF) and Magic Text-Encoder (MTE), as illustrated in Fig. 7. Given the prompt "A bud transforms into a yellow flower", the Group w/o MTE, can produce relatively better results. However, compared to the complete MagicTime, it still slightly lags in aspects such as fluency and degree of metamorphosis. The Group w/o MTF, due to the use of low-quality prompts, resulted in a decrease in generation quality, such as the appearance of strange buds in the middle of flowers. The Group w/o MA-S can generate the complete process, but as the dataset contains a large amount of watermark data, the results also include watermarks. The Group w/o MA-T struggles to effectively encode the concept of metamorphic, resulting in general video without metamorphic characteristics. The Group w/o DFE, similarly to the Group w/o MA-T, can not generate metamorphic video and has reduced generation quality due to the lack of metamorphic feature acquisition. We also conduct quantitative experiments, as shown in Fig. 6b, demonstrating that MagicTime significantly outperforms other methods across all four dimensions. The experimental settings are consistent with those in Section 4.4, and we finally collected 115 valid questionnaires. Our MagicTime significantly enhances metamorphic video generation. With simple adapters and training strategies, it validates the hypothesis that incorporating time-lapse videos into the model can encode more physical knowledge.

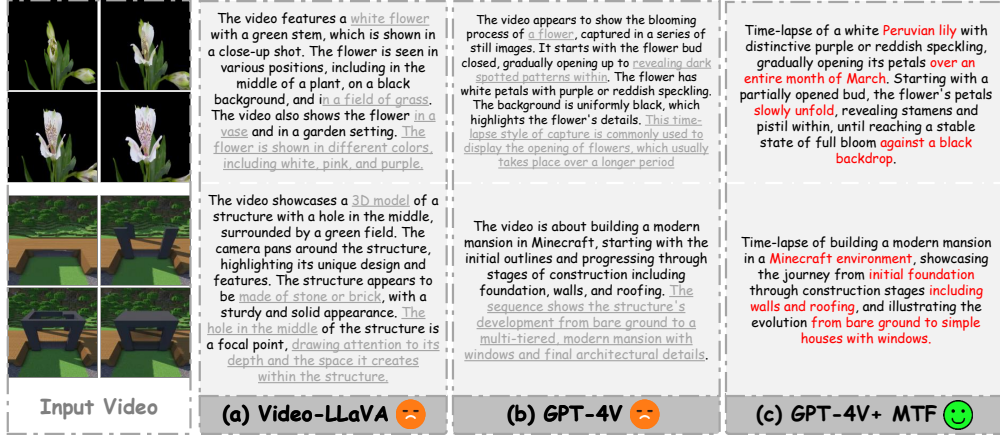


Figure 8: Effect of different large multimodal models and annotation strategies for the generated captions. Gray indicates inaccuracy or redundancy descriptions, red indicates precise or detailed descriptions. Text prompts exhibit clear temporal details, abundant object details, and smooth narrative flow when adopting GPT-4V and Multi-view Text Fusion.

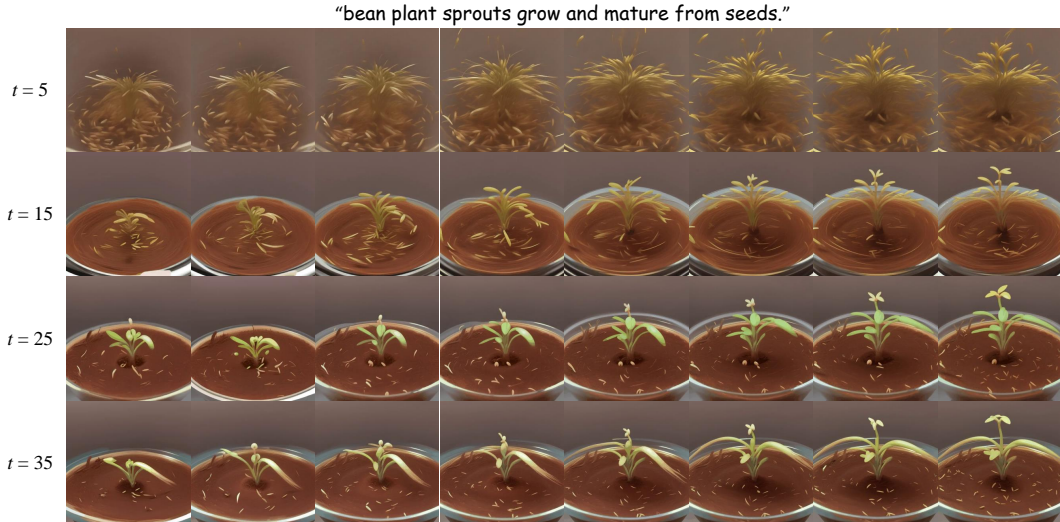


Figure 9: Effect of the number of inversion steps  $t$ . Best results are obtained when  $t = 25$ .

**Effect of the Enhanced Text Prompt** There are various methods for video captioning annotation. For example, 360DVD [54] employs BLIP [66], which is tailored for captioning tasks, while LanguageBind [57] uses the multimodal large model OFA [67]. However, we observe that both specialized and general models have limitations in comprehending metamorphic videos. We illustrate this by examining the leading multimodal large model Video-LLaVA [56], with results in Fig. 8. It shows Video-LLaVA struggles to capture fine-grained details and often produces irrelevant descriptions that may interfere with prompt instructions. Therefore, we choose GPT-4V for video annotation. Nevertheless, since GPT-4V only processes keyframes, it risks losing valuable information in the entire video. To mitigate this, we introduce Multi-view Text Fusion (MTF) to enhance the quality of video captions. GPT-4V with MTF can generate text prompts that are rich in temporal details, object specifics, and narrative coherence. We also apply MTF to Video-LLaVA; however, due to its limited ability to follow instructions, the improvements pre- and post-application are relatively minor.

**Effect of the Number of Inversion Steps** To assess the influence of the number of inversion steps, we conducted an ablation study to examine the effect of varying  $t$  (i.e., the number of inversion steps) during the inference stage of MagicTime. We set  $t = 5, 15, 25, 35$  and applied our approach to the ChronoMagic dataset to obtain metamorphic results. We evaluated Visual Quality (VQ), Frame



Figure 10: Examples of metamorphic time-lapse videos generated by our MagicTime-DiT based on Open-Sora-Plan v1.0.0 [70] with ChronoMagic-Landscape Dataset.

Consistency (FC), Metamorphic Amplitude (MA), and Text Alignment (TA) for each  $t$  value, with examples illustrated in Fig. 9 using *RcnzCartoon* as a representative case. In terms of VQ, we observed that when  $t$  is less than 25, the larger  $t$  is, the better VQ becomes. For FC, after  $t$  exceeds 5, there is good consistency throughout; for MA, when  $t$  equals 25, even if it is increased further, MA only shows minor changes; for TA, regardless of the value of  $t$ , it can always generate results that are aligned with a text prompt. When  $t$  is too small, the diffusion process lacks the necessary flexibility for significant changes, challenging effective generation. Conversely, a larger  $t$  value leads to extended reasoning times. In practice, we set  $t = 25$  to achieve best performance.

#### 4.6 Integrate MagicTime Scheme into DiT-based Architecture

Sora [68] is a text-to-video generation model released by OpenAI in February 2024, which shows the powerful potential of simulating the physical world. Due to OpenAI’s closed-source policy, the academic community is currently working on reproducing the open-source Sora-like structure based on the DiT (Diffusion-Transformer)-based Text-to-Video (T2V) generation framework [3, 69, 70]. The mission of this project is to help reproduce Sora and provide high-quality video-text data and data annotation pipelines, to support Open-Sora-Plan or other DiT-based T2V models. To this end, we take an initial step to integrate our MagicTime scheme into the DiT-based Framework. Specifically, our method supports the Open-Sora-Plan v1.0.0 [70] for fine-tuning. The Open-Sora-Plan v1.0.0 exhibits superior performance in generating landscape videos. Therefore, we first scale up with additional metamorphic landscape time-lapse videos in the same annotation framework to get the ChronoMagic-Landscape dataset. Then, we fine-tune the Open-Sora-Plan v1.0.0 with the ChronoMagic-Landscape dataset to get the MagicTime-DiT model. As shown in Fig. 10, our MagicTime-DiT has generated high-quality metamorphic landscape time-lapse videos. Now, we are still exploring to support more DiT-based T2V structures and continue on the road to scaling our ChronoMagic dataset, in hopes of truly bringing useful insights to the community.

## 5 Discussion and Conclusion

In this paper, we present MagicTime, a novel framework for metamorphic time-lapse video generation. It can generate metamorphic videos conforming to the content distribution and motion patterns in real-captured metamorphic videos. Extensive experiments demonstrate our effectiveness in generating high-quality metamorphic videos with various prompts and styles. Further, our MagicTime model and ChronoMagic benchmark can provide a simple yet effective solution for metamorphic video generation, which can facilitate further investigation by the community.

**Ethics Statement.** MagicTime can generate not only metamorphic videos with large time spans and high levels of realism but also high-quality general videos. Potential negative impacts exist as the technique can be used to generate fake video content for fraudulent purposes. We note that any technology can be misused.

## References

- [1] Yuwei Guo, Ceyuan Yang, Anyi Rao, Yaohui Wang, Yu Qiao, Dahua Lin, and Bo Dai. Animatediff: Animate your personalized text-to-image diffusion models without specific tuning. *arXiv preprint arXiv:2307.04725*, 2023.
- [2] Dan Kondratyuk, Lijun Yu, Xiuye Gu, José Lezama, Jonathan Huang, Rachel Hornung, Hartwig Adam, Hassan Akbari, Yair Alon, Vighnesh Birodkar, et al. Videopoet: A large language model for zero-shot video generation. *arXiv preprint arXiv:2312.14125*, 2023.
- [3] Xin Ma, Yaohui Wang, Gengyun Jia, Xinyuan Chen, Ziwei Liu, Yuan-Fang Li, Cunjian Chen, and Yu Qiao. Latte: Latent diffusion transformer for video generation. *arXiv preprint arXiv:2401.03048*, 2024.
- [4] Xiang Wang, Hangjie Yuan, Shiwei Zhang, Dayou Chen, Jiuniu Wang, Yingya Zhang, Yujun Shen, Deli Zhao, and Jingren Zhou. Videocomposer: Compositional video synthesis with motion controllability. *NeurIPS*, 36, 2024.
- [5] Jiuniu Wang, Hangjie Yuan, Dayou Chen, Yingya Zhang, Xiang Wang, and Shiwei Zhang. Modelscope text-to-video technical report. *arXiv preprint arXiv:2308.06571*, 2023.
- [6] Andreas Blattmann, Robin Rombach, Huan Ling, Tim Dockhorn, Seung Wook Kim, Sanja Fidler, and Karsten Kreis. Align your latents: High-resolution video synthesis with latent diffusion models. In *CVPR*, pages 22563–22575, 2023.
- [7] Hanzhuo Huang, Yufan Feng, Cheng Shi, Lan Xu, Jingyi Yu, and Sibe Yang. Free-bloom: Zero-shot text-to-video generator with llm director and ldm animator. *NeurIPS*, 36, 2024.
- [8] Wei Xiong, Wenhan Luo, Lin Ma, Wei Liu, and Jiebo Luo. Learning to generate time-lapse videos using multi-stage dynamic generative adversarial networks. In *CVPR*, pages 2364–2373, 2018.
- [9] Hongwei Xue, Bei Liu, Huan Yang, Jianlong Fu, Houqiang Li, and Jiebo Luo. Learning fine-grained motion embedding for landscape animation. In *Proceedings of the 29th ACM International Conference on Multimedia*, pages 291–299, 2021.
- [10] Piyush Sharma, Nan Ding, Sebastian Goodman, and Radu Soricut. Conceptual captions: A cleaned, hypernymed, image alt-text dataset for automatic image captioning. In *ACL*, Jan 2018.
- [11] Christoph Schuhmann, Romain Beaumont, Richard Vencu, Cade Gordon, Ross Wightman, Mehdi Cherti, Theo Coombes, Aarush Katta, Clayton Mullis, Mitchell Wortsman, et al. Laion-5b: An open large-scale dataset for training next generation image-text models. *NeurIPS*, 35:25278–25294, 2022.
- [12] Diederik P Kingma and Max Welling. Auto-encoding variational bayes. *arXiv preprint arXiv:1312.6114*, 2013.
- [13] Aaron Van Den Oord, Oriol Vinyals, et al. Neural discrete representation learning. *NeurIPS*, 30, 2017.
- [14] Danilo Jimenez Rezende and Shakir Mohamed. Variational inference with normalizing flows. *arXiv preprint arXiv*, May 2015.
- [15] Laurent Dinh, Jascha Sohl-Dickstein, and Samy Bengio. Density estimation using real nvp. *ICLR*, May 2016.
- [16] Weihao Xia, Yujiu Yang, Jing-Hao Xue, and Baoyuan Wu. Tedigan: Text-guided diverse face image generation and manipulation. In *CVPR*, pages 2256–2265, 2021.
- [17] Axel Sauer, Katja Schwarz, and Andreas Geiger. Stylegan-xl: Scaling stylegan to large diverse datasets. In *SIGGRAPH*, pages 1–10, 2022.
- [18] Axel Sauer, Tero Karras, Samuli Laine, Andreas Geiger, and Timo Aila. Stylegan-t: Unlocking the power of gans for fast large-scale text-to-image synthesis. *arXiv preprint:2301.09515*, 2023.

- [19] Chitwan Saharia, William Chan, Saurabh Saxena, Lala Li, Jay Whang, Emily L Denton, Kamyar Ghasemipour, Raphael Gontijo Lopes, Burcu Karagol Ayan, Tim Salimans, et al. Photorealistic text-to-image diffusion models with deep language understanding. *NeurIPS*, 35:36479–36494, 2022.
- [20] Aditya Ramesh, Mikhail Pavlov, Gabriel Goh, Scott Gray, Chelsea Voss, Alec Radford, Mark Chen, and Ilya Sutskever. Zero-shot text-to-image generation. In *ICML*, pages 8821–8831, 2021.
- [21] Aditya Ramesh, Prafulla Dhariwal, Alex Nichol, Casey Chu, and Mark Chen. Hierarchical text-conditional image generation with clip latents, 2022. *arXiv preprint:2204.06125*, 2022.
- [22] Dustin Podell, Zion English, Kyle Lacey, Andreas Blattmann, Tim Dockhorn, Jonas Müller, Joe Penna, and Robin Rombach. Sdxl: Improving latent diffusion models for high-resolution image synthesis. *arXiv preprint arXiv:2307.01952*, 2023.
- [23] Long Lian, Boyi Li, Adam Yala, and Trevor Darrell. Llm-grounded diffusion: Enhancing prompt understanding of text-to-image diffusion models with large language models. *arXiv preprint arXiv:2305.13655*, 2023.
- [24] Omer Bar-Tal, Lior Yariv, Yaron Lipman, and Tali Dekel. Multidiffusion: Fusing diffusion paths for controlled image generation. *ICML*, 2023.
- [25] Robin Rombach, Andreas Blattmann, Dominik Lorenz, Patrick Esser, and Bjorn Ommer. High-resolution image synthesis with latent diffusion models. In *CVPR*, Jun 2022.
- [26] Minghao Chen, Iro Laina, and Andrea Vedaldi. Training-free layout control with cross-attention guidance. In *CVPR*, pages 5343–5353, 2024.
- [27] Shihao Zhao, Dongdong Chen, Yen-Chun Chen, Jianmin Bao, Shaozhe Hao, Lu Yuan, and Kwan-Yee K Wong. Uni-controlnet: All-in-one control to text-to-image diffusion models. *NeurIPS*, 36, 2024.
- [28] Minghao Chen, Iro Laina, and Andrea Vedaldi. Training-free layout control with cross-attention guidance. In *CVPR*, pages 5343–5353, 2024.
- [29] Chong Mou, Xintao Wang, Liangbin Xie, Yanze Wu, Jian Zhang, Zhongang Qi, Ying Shan, and Xiaohu Qie. T2i-adapter: Learning adapters to dig out more controllable ability for text-to-image diffusion models. *arXiv preprint arXiv:2302.08453*, 2023.
- [30] Yujun Shi, Chuhui Xue, Jiachun Pan, Wenqing Zhang, Vincent YF Tan, and Song Bai. Dragdiffusion: Harnessing diffusion models for interactive point-based image editing. *arXiv preprint arXiv:2306.14435*, 2023.
- [31] Yuheng Li, Haotian Liu, Qingyang Wu, Fangzhou Mu, Jianwei Yang, Jianfeng Gao, Chunyuan Li, and Yong Jae Lee. Gligen: Open-set grounded text-to-image generation. In *CVPR*, 2023.
- [32] Max Bain, Arsha Nagrani, Gul Varol, and Andrew Zisserman. Frozen in time: A joint video and image encoder for end-to-end retrieval. In *ICCV*, 2021.
- [33] Yi Wang, Yanan He, Yizhuo Li, Kunchang Li, Jiashuo Yu, Xin Ma, Xinhao Li, Guo Chen, Xinyuan Chen, Yaohui Wang, et al. Internvid: A large-scale video-text dataset for multimodal understanding and generation. *arXiv preprint arXiv:2307.06942*, 2023.
- [34] Wenjing Wang, Huan Yang, Zixi Tuo, Huiguo He, Junchen Zhu, Jianlong Fu, and Jiaying Liu. Videofactory: Swap attention in spatiotemporal diffusions for text-to-video generation. *arXiv preprint arXiv:2305.10874*, 2023.
- [35] Uriel Singer, Adam Polyak, Thomas Hayes, Xi Yin, Jie An, Songyang Zhang, Qiyuan Hu, Harry Yang, Oron Ashual, Oran Gafni, et al. Make-a-video: Text-to-video generation without text-video data. *arXiv preprint arXiv:2209.14792*, 2022.
- [36] Andreas Blattmann, Tim Dockhorn, Sumith Kulal, Daniel Mendelevitch, Maciej Kilian, Dominik Lorenz, Yam Levi, Zion English, Vikram Voleti, Adam Letts, et al. Stable video diffusion: Scaling latent video diffusion models to large datasets. *arXiv preprint arXiv:2311.15127*, 2023.

- [37] Songwei Ge, Seungjun Nah, Guilin Liu, Tyler Poon, Andrew Tao, Bryan Catanzaro, David Jacobs, Jia-Bin Huang, Ming-Yu Liu, and Yogesh Balaji. Preserve your own correlation: A noise prior for video diffusion models. In *ICCV*, pages 22930–22941, 2023.
- [38] David Junhao Zhang, Jay Zhangjie Wu, Jia-Wei Liu, Rui Zhao, Lingmin Ran, Yuchao Gu, Difei Gao, and Mike Zheng Shou. Show-1: Marrying pixel and latent diffusion models for text-to-video generation. *arXiv preprint arXiv:2309.15818*, 2023.
- [39] Weimin Wang, Jiawei Liu, Zhijie Lin, Jiangqiao Yan, Shuo Chen, Chetwin Low, Tuyen Hoang, Jie Wu, Jun Hao Liew, Hanshu Yan, et al. Magicvideo-v2: Multi-stage high-aesthetic video generation. *arXiv preprint arXiv:2401.04468*, 2024.
- [40] Omer Bar-Tal, Hila Chefer, Omer Tov, Charles Herrmann, Roni Paiss, Shiran Zada, Ariel Ephrat, Junhwa Hur, Yuanzhen Li, Tomer Michaeli, et al. Lumiere: A space-time diffusion model for video generation. *arXiv preprint arXiv:2401.12945*, 2024.
- [41] Seonghyeon Nam, Chongyang Ma, Menglei Chai, William Brendel, Ning Xu, and Seon Joo Kim. End-to-end time-lapse video synthesis from a single outdoor image. In *CVPR*, pages 1409–1418, 2019.
- [42] Hongwei Xue, Bei Liu, Huan Yang, Jianlong Fu, Houqiang Li, and Jiebo Luo. Learning fine-grained motion embedding for landscape animation. In *ACM MM*, pages 291–299, 2021.
- [43] Jiangning Zhang, Chao Xu, Liang Liu, Mengmeng Wang, Xia Wu, Yong Liu, and Yunliang Jiang. Dtvnet: Dynamic time-lapse video generation via single still image. In *ECCV*, pages 300–315, 2020.
- [44] Yuki Endo, Yoshihiro Kanamori, and Shigeru Kuriyama. Animating landscape: self-supervised learning of decoupled motion and appearance for single-image video synthesis. *arXiv preprint arXiv:1910.07192*, 2019.
- [45] Jonathan Ho, Ajay Jain, and Pieter Abbeel. Denoising diffusion probabilistic models. *NeurIPS*, 33:6840–6851, 2020.
- [46] Jiaming Song, Chenlin Meng, and Stefano Ermon. Denoising diffusion implicit models. *arXiv preprint arXiv*, Oct 2020.
- [47] Shaofeng Zhang, Jinfa Huang, Qiang Zhou, Zhibin Wang, Fan Wang, Jiebo Luo, and Junchi Yan. Continuous-multiple image outpainting in one-step via positional query and a diffusion-based approach. *arXiv preprint arXiv:2401.15652*, 2024.
- [48] Gary Bradski, Adrian Kaehler, et al. *Opencv. Dr. Dobb’s journal of software tools*, 3(2), 2000.
- [49] Alec Radford, Jong Wook Kim, Chris Hallacy, Aditya Ramesh, Gabriel Goh, Sandhini Agarwal, Girish Sastry, Amanda Askell, Pamela Mishkin, Jack Clark, et al. Learning transferable visual models from natural language supervision. In *ICML*, pages 8748–8763, 2021.
- [50] Tom Brown, Benjamin Mann, Nick Ryder, Melanie Subbiah, Jared D Kaplan, Prafulla Dhariwal, Arvind Neelakantan, Pranav Shyam, Girish Sastry, Amanda Askell, et al. Language models are few-shot learners. *NeurIPS*, 33:1877–1901, 2020.
- [51] Josh Achiam, Steven Adler, Sandhini Agarwal, Lama Ahmad, Ilge Akkaya, Florencia Leoni Aleman, Diogo Almeida, Janko Altenschmidt, Sam Altman, Shyamal Anadkat, et al. Gpt-4 technical report. *arXiv preprint arXiv:2303.08774*, 2023.
- [52] Hanjia Lyu, Jinfa Huang, Daoan Zhang, Yongsheng Yu, Xinyi Mou, Jinsheng Pan, Zhengyuan Yang, Zhongyu Wei, and Jiebo Luo. Gpt-4v (ision) as a social media analysis engine. *arXiv preprint arXiv:2311.07547*, 2023.
- [53] Tim Dettmers, Artidoro Pagnoni, and Holtzman. Qlora: Efficient finetuning of quantized llms. *NeurIPS*, 36, 2024.
- [54] Qian Wang, Weiqi Li, Chong Mou, Xinhua Cheng, and Jian Zhang. 360dvd: Control-able panorama video generation with 360-degree video diffusion model. *arXiv preprint arXiv:2401.06578*, 2024.

- [55] Ze Ma, Daquan Zhou, Chun-Hsiao Yeh, Xue-She Wang, Xiuyu Li, Huanrui Yang, Zhen Dong, Kurt Keutzer, and Jiashi Feng. Magic-me: Identity-specific video customized diffusion. *arXiv preprint arXiv:2402.09368*, 2024.
- [56] Bin Lin, Bin Zhu, Yang Ye, Munan Ning, Peng Jin, and Li Yuan. Video-llava: Learning united visual representation by alignment before projection. *arXiv preprint arXiv:2311.10122*, 2023.
- [57] Bin Zhu, Bin Lin, Munan Ning, Yang Yan, Jiayi Cui, HongFa Wang, Yatian Pang, Wenhao Jiang, Junwu Zhang, Zongwei Li, et al. Languagebind: Extending video-language pretraining to n-modality by language-based semantic alignment. *arXiv preprint arXiv:2310.01852*, 2023.
- [58] Xu Duo. Makelongvideo. In *Github*, 2023.
- [59] Haoxin Chen, Yong Zhang, Xiaodong Cun, Menghan Xia, Xintao Wang, Chao Weng, and Ying Shan. Videocrafter2: Overcoming data limitations for high-quality video diffusion models. *arXiv preprint arXiv:2401.09047*, 2024.
- [60] Spencer Sterling. zeroscope. In *Huggingface*, 2023.
- [61] Yaohui Wang, Xinyuan Chen, Xin Ma, Shangchen Zhou, Ziqi Huang, Yi Wang, Ceyuan Yang, Yinan He, Jiashuo Yu, Peiqing Yang, et al. Lavie: High-quality video generation with cascaded latent diffusion models. *arXiv preprint arXiv:2309.15103*, 2023.
- [62] Levon Khachatryan, Andranik Movsisyan, Vahram Tadevosyan, Roberto Henschel, Zhangyang Wang, Shant Navasardyan, and Humphrey Shi. Text2video-zero: Text-to-image diffusion models are zero-shot video generators. *arXiv preprint arXiv:2303.13439*, 2023.
- [63] Martin Heusel, Hubert Ramsauer, Thomas Unterthiner, Bernhard Nessler, and Sepp Hochreiter. Gans trained by a two time-scale update rule converge to a local nash equilibrium. *NeurIPS*, Jan 2017.
- [64] Thomas Unterthiner, Sjoerdvan Steenkiste, Karol Kurach, Raphaël Marinier, Marcin Michalski, and Sylvain Gelly. Fvd: A new metric for video generation. *ICLR*, Mar 2019.
- [65] Chenfei Wu, Lun Huang, Qianxi Zhang, Binyang Li, Lei Ji, Fan Yang, Guillermo Sapiro, and Nan Duan. Godiva: Generating open-domain videos from natural descriptions. *arXiv preprint arXiv:2104.14806*, 2021.
- [66] Junnan Li, Dongxu Li, Silvio Savarese, and Steven Hoi. Blip-2: Bootstrapping language-image pre-training with frozen image encoders and large language models. In *ICML*, pages 19730–19742, 2023.
- [67] Peng Wang, An Yang, Rui Men, Junyang Lin, Shuai Bai, Zhikang Li, Jianxin Ma, Chang Zhou, Jingren Zhou, and Hongxia Yang. Ofa: Unifying architectures, tasks, and modalities through a simple sequence-to-sequence learning framework. In *ICML*, pages 23318–23340, 2022.
- [68] Tim Brooks, Bill Peebles, Connor Holmes, Will DePue, Yufei Guo, Li Jing, David Schnurr, Joe Taylor, Troy Luhman, Eric Luhman, Clarence Ng, Ricky Wang, and Aditya Ramesh. Video generation models as world simulators. 2024.
- [69] Zangwei Zheng, Xiangyu Peng, and Yang You. Open-sora: Democratizing efficient video production for all. In *Github*, March 2024.
- [70] Bin Lin, Shenghai Yuan, Zhenyu Tang, Junwu Zhang, Xinhua Cheng, Liuhan Chen, Yang Ye, Bin Zhu, Yunyang Ge, Xing Zhou, Shaoling Dong, Yemin Shi, Yonghong Tian, and Li Yuan. Tinsora. In *Github*, March 2023.
- [71] Haonan Qiu, Menghan Xia, Yong Zhang, Yingqing He, Xintao Wang, Ying Shan, and Ziwei Liu. Freenoise: Tuning-free longer video diffusion via noise rescheduling. *arXiv preprint arXiv:2310.15169*, 2023.
- [72] Zhen Li, Zuo-Liang Zhu, Ling-Hao Han, Qibin Hou, Chun-Le Guo, and Ming-Ming Cheng. Amt: All-pairs multi-field transforms for efficient frame interpolation. In *CVPR*, pages 9801–9810, 2023.

## A Additional Experimental Results

### A.1 Pseudo Long Video Generation

Current text-to-video (T2V) models [40, 3, 1, 54] often face challenges in generating 16-frame videos, which typically feature only camera motion. The generation of longer videos [71] commonly involves multiple forward inferences based on a 16-frame model, followed by concatenating the results. Since our method can produce metamorphic videos within 16 frames, it effectively compresses the content of a longer video into 16 frames. Consequently, combining a frame interpolation model with the outputs of MagicTime can theoretically achieve the effects of longer video generation. We hope this insight will inspire and advance future research in this burgeoning field. We present some examples using the interpolation model [72], as illustrated in Fig. 12. It is evident that with MagicTime’s capability for metamorphic generation, pseudo-long videos can be produced.

### A.2 Resolution Scalability

Resolution scalability is a significant attribute of the T2V model with a U-Net architecture. To assess whether MagicTime retains this feature, we conducted related experiments, as depicted in Fig. 13. Despite being trained at a resolution of  $512 \times 512$ , our method demonstrates remarkable generalization capabilities across a wide range of resolutions. This scalability is particularly prominent when our model is applied to higher resolutions such as  $1024 \times 1024$ , where it maintains high fidelity and consistency in generated details. Similarly, at lower resolutions, such as  $128 \times 128$  and  $256 \times 256$ , our method preserves structural integrity and aesthetic quality. This robust generalization may be attributed to the inherent properties of the underlying generative model, Stable Diffusion [25], which we employ in our framework.

### A.3 More Cases on Metamorphic Videos

Due to space constraints, we present additional metamorphic videos generated by MagicTime and other baseline methods in Fig. 14 and Fig. 16. It is clear that MagicTime consistently surpasses existing state-of-the-art Time-to-Video (T2V) models across various scenarios, from melting ice to the expansion of bread. This highlights MagicTime’s adeptness in capturing physical phenomena such as expansion, melting, and burning. Furthermore, our approach consistently yields expected results and demonstrates robust generalization capabilities across diverse DreamBooths, from RealisticVision and ToonYou to RcnzCartoon. Fig. 17 showcases samples from the dataset, which primarily consists of metamorphic time-lapse videos of plants, buildings, ice, food, and other categories.

### A.4 More Hyperparameter Analysis

In the Cascade Preprocessing module, we employ OpenCV to detect video transitions based on the grayscale difference between two frames. The choice of the difference threshold  $\theta$  significantly impacts OpenCV’s ability to identify transitions. Therefore, we conducted ablation experiments

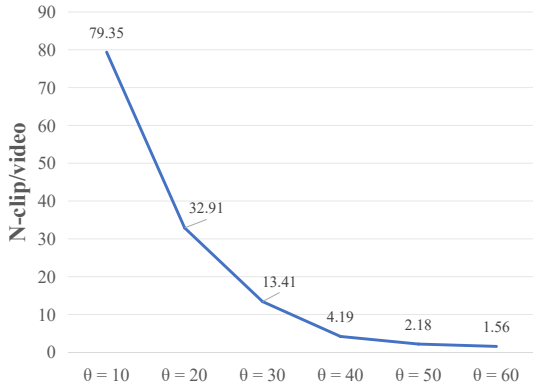


Figure 11: Ablation on the settings of  $\theta$ . Best results are obtained when  $\theta = 40$ .



Figure 12: **Pseudo Long Video Generation.** Our method can be converted to a long video generation model by using an interpolation model [72].

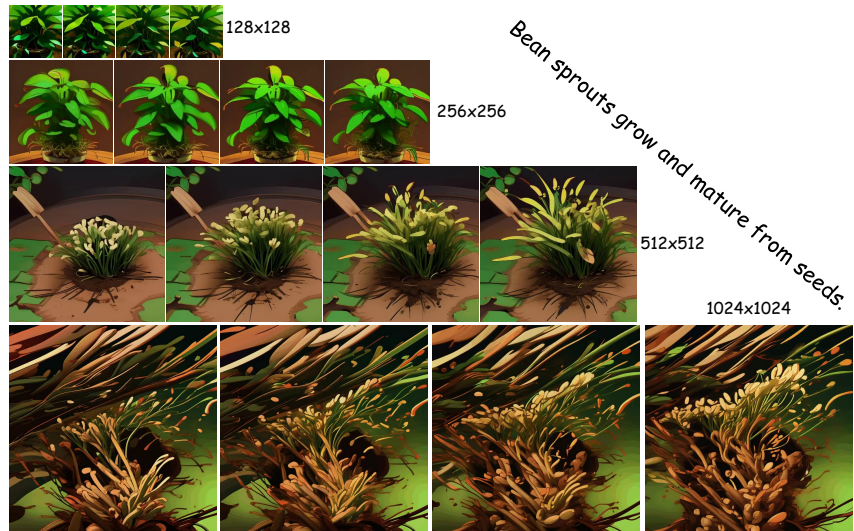


Figure 13: **Resolution Scalability.** The results demonstrate the generalization of our method.

with varying  $\theta$  values to find optimal values, as depicted in Fig. 11. The actual average number of transitions is approximately six. When  $\theta$  is too large, many frames are erroneously identified as transitions. Conversely, when  $\theta$  is too small, it results in missed detections. It can be seen that optimal results are achieved when  $\theta$  is set to 40.

### A.5 Questionnaire Visualization

To enhance the reliability of the experiment, we developed both coarse-grained and fine-grained questionnaires during the data collection phase and invited 200 participants to provide their responses. The coarse-grained questionnaire required participants to assess these four criteria and select the video that best met their requirements, as shown in Fig. 15a. As this questionnaire was more user-friendly, a total of 300 questionnaires were collected for all surveys related to this work. The fine-grained questionnaire asked participants to evaluate the visual quality, frame consistency, metamorphic amplitude, and text alignment of each video set, as shown in Fig. 15b.

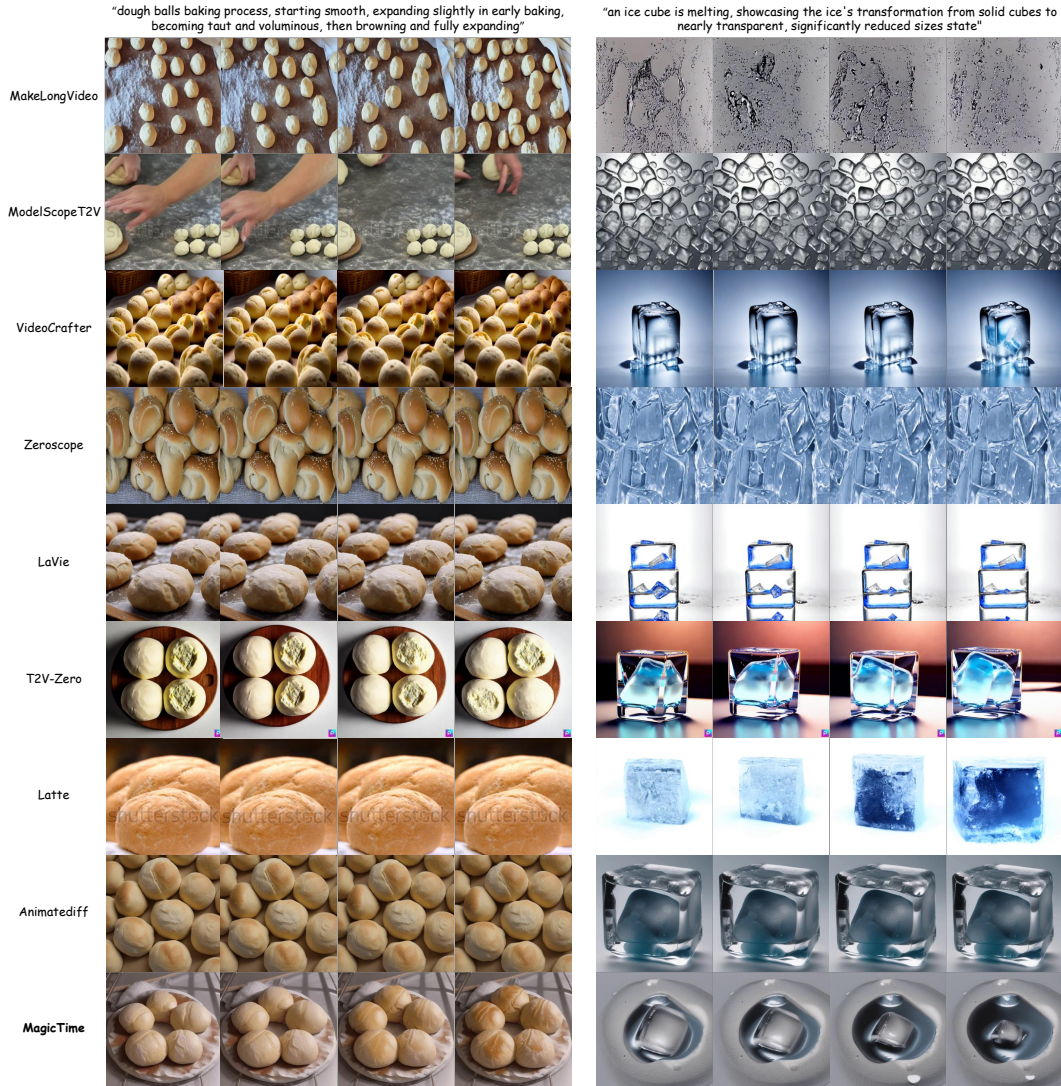


Figure 14: **More qualitative comparison of metamorphic video generation.** MagicTime achieves better results compared to the current leading T2V models.

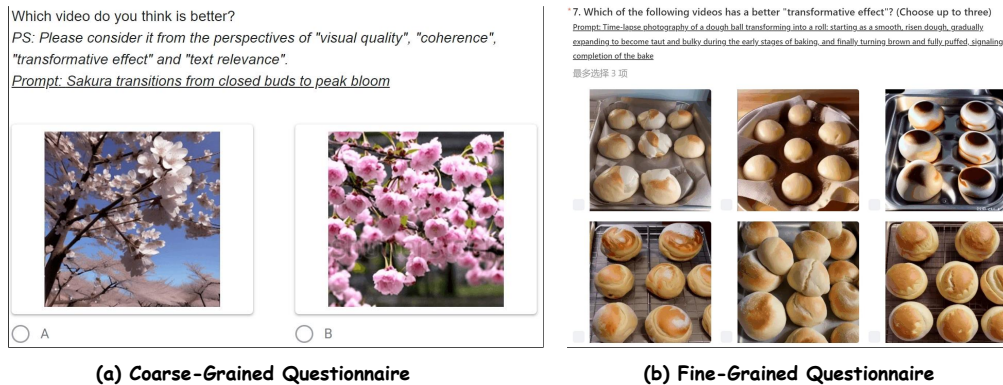


Figure 15: **Visualization of the Questionnaire for Human Evaluation.**

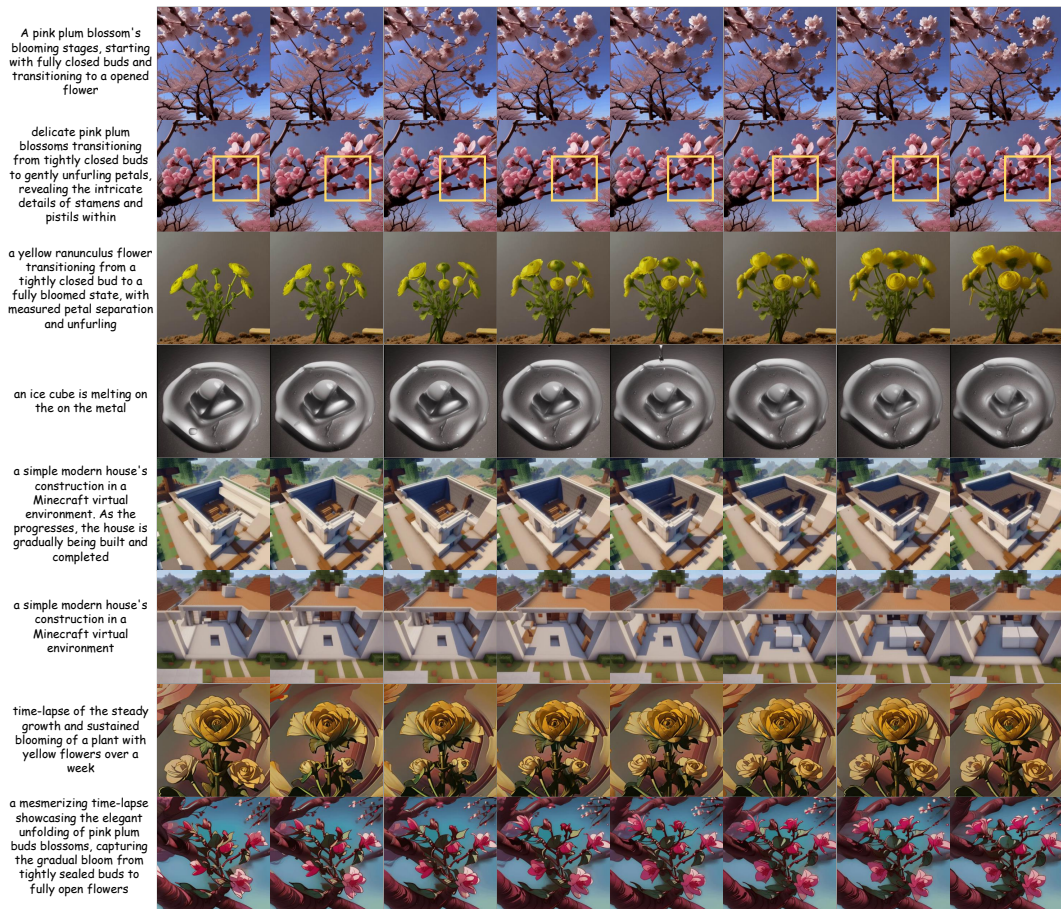


Figure 16: More examples of our approach applied to generated metamorphic videos. Metamorphic videos categories include *RealisticVision* (Row 1-4), *RenzCartoon* (Row 5-6) and *ToonYou* (Row 7-8). Even with a large state amplitude, the quality, consistency, and semantic relevance of generated videos are excellent.

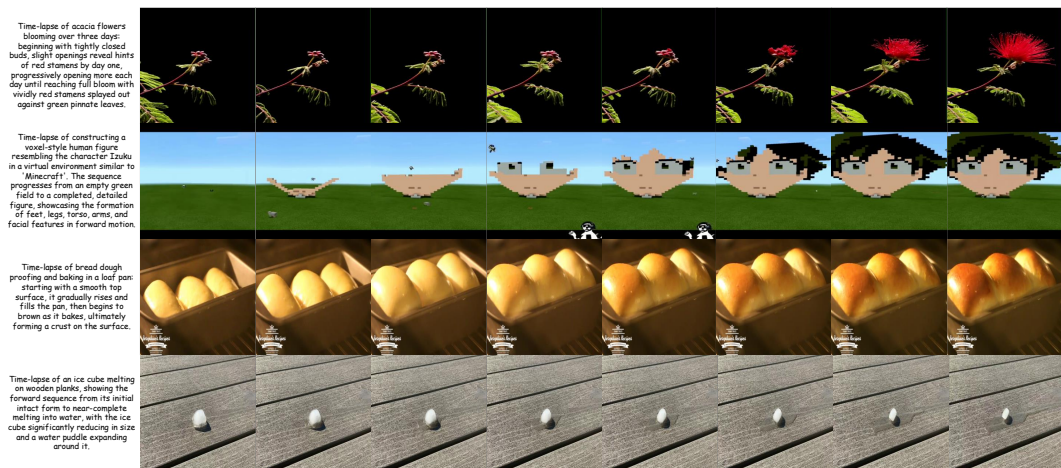


Figure 17: Samples from the ChronoMagic dataset. The dataset consists of metamorphic time-lapse videos, which exhibit physical knowledge, long persistence, and strong variation.